International Journal Multidisciplinary
Homepage : https://journal.antispublisher.com/index.php/IJMI
Email : admin@antispublisher.com

e-ISSN : 3031-9870
IJMI, Vol. 3, No. 2, May 2026
Page 376-394

Studying the Influence of The Length of Terminal Thioalkyl Groups on The Liquid Crystalline Properties of Imine-Ester Benzothiazole

Nizar S. Nwyr[1], Uhood J. Al-Hamdani[2], Tahseen A. Alsalim[3]
[1,2,3]University of Basrah, Iraq

DOI : https://doi.org/10.61796/ijmi.v3i2.479

Sections Info

Article history:
Submitted: March 15, 2026
Final Revised: April 05, 2026
Accepted: April 20, 2026
Published: May 06, 2026

Keywords:
6-fluorobenzothiazole
Thioalkyl
Imine-Ester linkages
Liquid crystal
DFT calculations

ABSTRACT

Objective: *A chain of new calamitic liquid crystals, featuring a heterocyclic (benzothiazole) core structure with two phenyl rings, a terminal thioalkyl string, and azomethene and ester linkages, were synthesized and described. This chain comprises of seven compounds, differentiated by the length of the thioalkyl string (-SRn, n = 1, 2, 4–8).* ***Method:*** *The results of the spectral study aligned with the anticipated structure. The structures of synthesized compounds were verified via various spectroscopic methods, including 1H-NMR, 13C-NMR, mass spectrometry, and FT-IR spectroscopy. Differential scanning calorimetry (DSC) and polarizing optical microscopy (POM) have been utilized to confirm their mesomorphic properties. Theoretical computations were performed via the density functional theory (DFT) approach at the CAM-B3LYP/6-311G (2d,p) level.* ***Results:*** *Only the nematic phase was noticed for the first and second compounds of the chain (n = 1, 2). With the increase length of the thioalkyl chain to n = 4, 5, 6, the nematic phase emerged alongside an extra smectic phase. Upon transitioning from n = 7 to the maximum compound n = 8, the nematic phase vanished, and these members alone displayed the Smectic phase (SmA). (DFT) data were correlated with empirical data from liquid crystalline studies, revealing that the molecular architecture, reactivity, dipole moment, aspect ratio, and polarizability of the examined members are significantly influenced by the length of the terminal chain.* ***Novelty:*** *A chain of new calamitic liquid crystals, featuring a heterocyclic (benzothiazole) core structure with azomethene and ester linkages and a terminal thioalkyl string, were synthesized and described, with properties significantly influenced by the length of the terminal chain.*

INTRODUCTION

Liquid crystals (LCs) are a distinct Subcategory between the continuum of solid and liquid phases of [1-4]. Liquid crystal, or mesomorphic state, exhibits feature that combine those of crystals and liquids, displaying distinctive photoelectric characteristics not found in either [1]. Calamitic or discotic molecules were originally essential in the advancement of traditional thermotropic mesomorphic [5]. The mesomorphic behavior of a calamitic mesogenic essentially depend on its molecular structure, where even little modifications in molecular geometry can result in substantial alterations in its mesomorphic characteristics. A comprehensive examination in this domain has resulted in several empirical principles, especially those pertains to the effect of molecular composition on the manifestation of nematic and smectic phases [6,7]. It is widely recognized that the mesomorphic characteristics of rod-like mesogenic can be significantly affected by the structural modification of terminal groups, such as alkyloxy, alkyl , and thioalkyl flocks [8-12]. This may affect the varieties of mesophases and melting points, among other factors. [13-18]. calamitic mesogenic typically comprise one or more

ring molecules, including aromatic, heterocyclic, and aliphatic rings, which are interconnected or joined by suitable connections to form certain rigid structures [19, 20]. A significant number of phenyl compounds incorporating heterocyclic components have been prepared, and a passion in this composition is steadily growing [21-23]. The heterocyclic unit typically has a five - or six- membered ring including atoms of hetero such as S, O, and N, as these atoms have a greater ability to be polarized than carbon. [23]. Consequently, these atoms can alter the mesomorphic phase and physical characteristics of the target phase [24]. Research on heterocyclic liquid crystal materials has markedly increased in recent years due to the diversity of their applications. The preliminary report on a nematic benzothiazole was presented by Vorlander [25]. Uhood et al. reported innovative ester compounds, including a thioalkyl series at the terminal position of the benzene ring [26]. Nematic mesophases produced by these rod-like substances were observed. Prajapati and Bundy [27] documented the use of two mesogenic homologous chains that differ in the length of the alkoxy chain, using benzothiazole ring systems substituted at position 6, including a basic azo bond. K.-L. Foo et al. [28] discovered a chain of novel calamitic compounds consisting of a heterocyclic (benzothiazole) moiety and a terminal alkoxy chain. Nematic and/or smectic phases were observed. Liquid crystal materials have recently demonstrated extensive technical uses, including displays [29, 30], optical transistors [31, 32], and biological molecule fluorescence sensors [33,34]. These attributes stem from their ability to create linear or lateral dipoles and geometric arrangements. [35-37]. Electronegative heteroatoms (O, N, and S) significantly affect bond angles, resonance delocalization, and molecular structure [38-45]. The growing scientific attention in the production of heterocyclic mesomorphic has led us to prepare a series of novel 6-fluoro-benzothiazole-based compounds. This study elucidates the synthesis and mesomorphic properties of a homologous series of heterocyclic liquid crystals, varying in terminal chain length (n = 1, 2, 4-8), as depicted in (Figure 1). The targeted compounds comprise a thioalkyl tail, ester and azomethene linkages, two phenyl groups, and one benzothiazole moiety. We want to theoretically substantiate our actual outcomes via the (DFT) technique and elucidate the impact of including a terminal thioalkyl chain into the molecule.

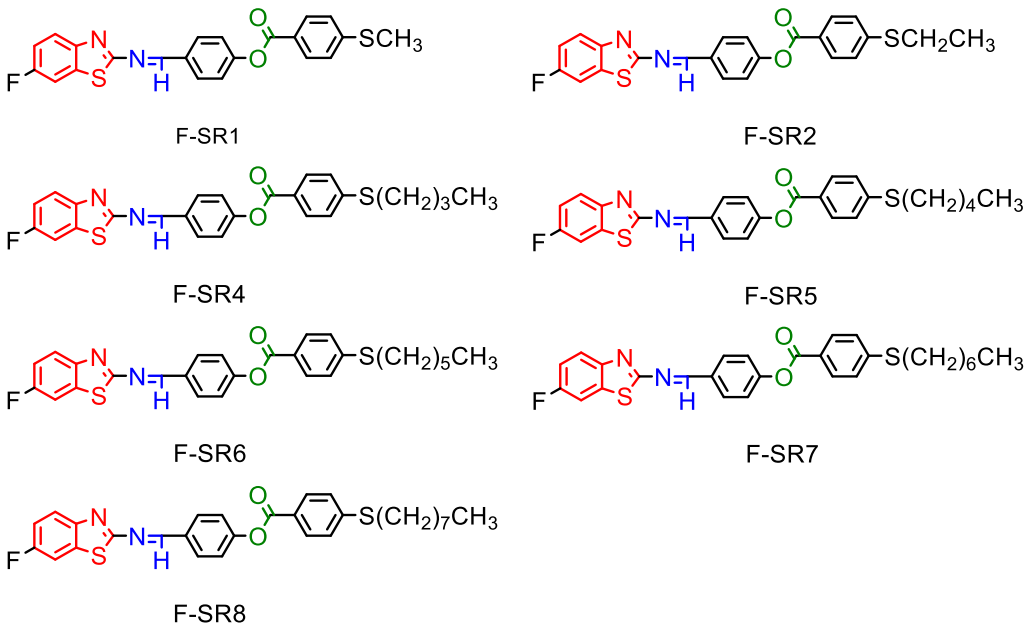

Figure 1. Chemical structures of the synthesized compounds.

RESEARCH METHOD

Experimental

Instrumentation

An FT-IR-8400S device (Japan type, Shimadzu) in the shape of a potassium bromide disc was used to obtain infrared spectra in the range of 400–4000 cm^{-1}. Using $CDCl_3$ and DMSO as solvents and TMS as an internal standard, ^{1}H-NMR and ^{13}C-NMR spectra were obtained using a Bruker apparatus. Using a heating rate of 10°C min^{-1}, the mesomorphic and isotropic phase transition temperatures were measured using a DSC device of type (NETZSCH DSC 204 F1) for the compound (F-SR1) and a DSC device of type (DSC-60 SHIMADZU) for the compounds F-SR2, F-SR4, F-SR5, F-SR6, F-SR7, and F-SR8A Leitz Labor Lux 12 Pol optical microscope with polarized light and a Leitz 350 hot stage (Germany) equipped with a Vario-Orthomat were used to identify phase transitions. For the substances F-SR2, F-SR5, F-SR6, F-SR7, and F-SR8, mass spectra were acquired using an electrospray ionization mass spectrometry (ESI-MS) Shimadzu LCMS 2010 A apparatus. For the substances F-SR1 and F-SR4, mass spectra were acquired using an Agilent Technologies 5975C mass spectrometer equipped with EI technology.

Synthesis procedures of thioalkyl benzoic acid

Upon dissolving 0.001 mol (0.154 g) of 4-mercaptobenzoic acid in 20 mL of ethanol, 0.002 mol (0.276 g) of potassium carbonate was subsequently introduced to it. The amalgamation was situated in a round-bottom flask and subjected to constant agitation. Subsequently, at ambient temperature, 0.001 mol (0.137 g) of the corresponding alkyl bromide (RBr) was introduced. Reflux distillation was conducted for an entire day. Following the reaction, ethanol was evaporated, and 20 mL of distilled water was introduced to the resultant precipitate. Subsequent to heating the combination, it was permitted to cool to ambient temperature. Concentrated hydrochloric acid was employed

to acidify the solution, resulting in the formation of a white precipitate that was subsequently filtered and thoroughly rinsed with distilled water. According to scheme 1, it was refined through recrystallization from absolute ethanol [26,46].

Synthesis procedures of Schiff bases

In a round flask, 0.001 mol of (p-formylphenol) was separately added and dissolved in 10 mL of ethanol. Subsequently, 0.001 mol of 6-fluorobenzo[d]thiazol-2-amine was introduced, along with 2-3 drops of glacial acetic acid. The combination was subjected to reflux for 3 hours, after which it was allowed to evaporate the ethanol, resulting in the formation of yellow crystals. These crystals were purified through recrystallization using absolute ethanol [47,48], according to the scheme (1).

Synthesis procedures of Ester

Benzoic acid derivatives (0.001 mol), 4- (((6- fluorobenzo [d] thiazol- 2-yl) imino) methyl) phenol (0.001 mol), N,N′-Dicyclohexyl carbodiimide (DCC) (0.001 mol, 0.206 g), and 4-Dimethylaminopyridine (DMAP) (0.001 mol, 0.122 g) were dissolved in 1,2- dichloromethane (DCM) in a round-bottom flask. N,N'- dicyclohexyl urea (DHU), a by-product with a melting point of 232–233°C, was produced following the finished of the addition and subsequent continuous stirring of the reaction at room temperature for a whole day. Following the filtration of the combination, the solvent was permitted to evaporate from the filtrate. The product, depicted in Scheme (1), was acquired as a yellow hurried and then purified via recrystallization using absolute ethanol [49–52].

(E)-4-(((6-fluorobenzo[d]thiazol-2-yl)imino) methyl)phenyl4-(methylthio)benzoate(F-SR1):

Chemical Formula: $C_{22}H_{15}FN_2O_2S_2$, yellow solid, yield :74 %; ^{1}H-NMR (400 MHz, $CDCl_3$) δ ppm: 2.55 (S, 3H, - S$\underline{CH_3}$) ppm, 7.19-8.11 (m, 11H, Ar-H) ppm, 9.05 ppm (S, 1H, CH=N) (Figure 2,a) ; ^{13}C-NMR (400 MHz, $CDCl_3$) δ ppm: 14.77 ppm (-S$\underline{CH_3}$), 107.87-159.13 ppm (Ar-C), 161.57 ppm (CH=N), 164.81 ppm (C=O ester), 171.23 ppm (C=N thiazole) (Figure 2,b) ; IR (cm^{-1}): 3053 (C-H aromatic), 2858-2987 (C-H aliphatic), 1730 (C=O ester), 1593 (CH=N), 1577 (C=N thiazole) (Figure 2,c) ; MS (EI *m/z*) 422.2 [M^+] (Figure 2,d).

(E)-4-(((6- fluorobenzo[d]thiazol-2-yl)imino) methyl)phenyl 4-(ethylthio)benzoate (F-SR2):

Chemical Formula: $C_{23}H_{17}FN_2O_2S_2$, yellow solid, yield: 73.5 %; ^{1}H-NMR (400 MHz, DMSO) δ ppm: 1.27-1.30 (t,3H, $\underline{CH_3}$) ppm, 3.06-3.11 (q,2H, - SCH_2) ppm, 7.01-8.04 (m,11H,Ar-H) ppm, (9.05) (S,1H, CH=N) ppm; ^{13}C-NMR (400 MHz, DMSO) δ ppm: 14.25 ppm ($\underline{CH_3}$), 25.26 ppm (-SCH_2), 108.09-156.45 ppm (Ar-C), 158.80 ppm (CH=N), 164.39 ppm (C=O ester), 166.93 ppm (C=N thiazole); IR (cm^{-1}): 3057 (C-H aromatic), 2873-2976 (C-H aliphatic), 1732 (C=O ester), 1598 (CH=N), 1573 (C=N thiazole); MS (ESI *m/z*) 437 [M^+].

(E)-4- (((6- fluorobenzo[d]thiazol-2-yl)imino) methyl)phenyl 4-(butylthio)benzoate (F-SR4):

Chemical Formula: $C_{25}H_{21}FN_2O_2S_2$, yellow solid, yield:75 %; ^{1}H-NMR (400 MHz, $CDCl_3$) δ ppm: 0.95-0.98 (t, 3H, $\underline{CH_3}$) ppm, 1.46-1.55 (H,2H, -S $(CH_2)_2\underline{CH_2}CH_3$) ppm,

1.68-1.75 (P,2H, -S $CH_2\underline{CH_2}$ CH_2CH_3) ppm, 3.00-3.04 (t,2H, -$SCH_2(CH_2)_2CH_3$) ppm, 7.18-8.11 (m,11H,Ar-H) ppm, 9.06 (S,1H, CH=N) ppm; ^{13}C-NMR (400 MHz, $CDCl_3$) δ ppm:13.66 ppm ($\underline{CH_3}$), 22.07 ppm (-S $(CH_2)_2\underline{CH_2}CH_3$), 30.74 ppm (-$SCH_2\underline{CH_2}CH_2CH_3$), 31.57 ppm (-$SCH_2(CH_2)_2CH_3$), 107.91-159.12 ppm (Ar-C), 161.56 ppm (CH=N),164.87 ppm (C=O ester), 171.24 ppm (C=N thiazole); IR (cm^{-1}): 3057 (C-H aromatic), 2873-2956 (C-H aliphatic), 1732 (C=O ester), 1597 (CH=N), 1573 (C=N thiazole); MS (EI *m/z*) 464.4 [M^+].

(E)-4-(((6-fluorobenzo[d]thiazol-2-yl)imino) methyl)phenyl 4-(pentylthio)benzoate (F-SR5):

Chemical Formula: $C_{26}H_{23}FN_2O_2S_2$, yellow solid, yield: 76.5 %; ^{1}H-NMR (400 MHz, DMSO) δ ppm: 0.86-0.89 (t,3H, $\underline{CH_3}$) ppm, 1.29-1.39 (H,2H, -$S(CH_2)_3\underline{CH_2}CH_3$) ppm,1.41-1.44 (P,2H, -$S(CH_2)_2\underline{CH_2}$ CH_2CH_3) ppm, 1.61-1.68 (p,2H, -$SCH_2\underline{CH_2}$ $(CH_2)_2CH_3$) ppm, 3.07-3.11 (t,2H,-$SCH_2(CH_2)_3CH_3$) ppm, 7.37-8.21 (m,11H,Ar-H) ppm, 9.21 (S,1H, CH=N, a) ppm; ^{13}C-NMR (400 MHz, $CDCl_3$) δ ppm:13.97 ppm ($\underline{CH_3}$), 22.26 ppm (-$S(CH_2)_3\underline{CH_2}CH_3$), 28.38 ppm (-$S(CH_2)_2\underline{CH_2}CH_2CH_3$), 31.08 ppm (-$SCH_2\underline{CH_2}$ $(CH_2)_2CH_3$), 31.85 ppm (-$SCH_2(CH_2)_3CH_3$), 107.91-159.11 ppm (Ar-C), 161.56 ppm (CH=N),164.87 ppm (C=O ester), 171.23 ppm (C=N thiazole); IR (cm^{-1}): 3057 (C-H aromatic), 2860-2956 (C-H aliphatic), 1732 (C=O ester), 1597 (CH=N), 1573 (C=N thiazole); MS (ESI *m/z*) 479 [M^+].

(E)-4-(((6- fluorobenzo[d]thiazol-2-yl)imino) methyl)phenyl 4-(hexylthio)benzoate (F-SR6):

Chemical Formula: $C_{27}H_{25}FN_2O_2S_2$, yellow solid, yield:75.7 %; ^{1}H-NMR (400 MHz, $CDCl_3$) δ ppm: 0.88-0.92 (t,3H, $\underline{CH_3}$) ppm, 1.32-1.34 (m,4H, -$S(CH_2)_3\underline{(CH_2)_2}CH_3$) ppm, 1.45-1.49 (P,2H, -$S(CH_2)_2$ $\underline{CH_2}$ $(CH_2)_2CH_3$) ppm, 1.65-1.74 (p,2H, -SCH_2 $\underline{CH_2}$ $(CH_2)_3CH_3$) ppm, 3.00-3.03 (t,2H,-$SCH_2CH_2(CH_2)_4CH_3$), 7.19-8.11 (m,11H,Ar-H), 9.05 (S,1H, CH=N, a); ^{13}C-NMR (400 MHz, $CDCl_3$) δ ppm: 14.01 ppm ($\underline{CH_3}$),22.53 ppm (-$S(CH_2)_4\underline{CH_2}$ CH_3), 28.60 ppm (-$S(CH_2)_3\underline{CH_2}$ CH_2 CH_3), 28.66 ppm (-$S(CH_2)_2\underline{CH_2}$ $(CH_2)_2$ CH_3), 31.34 ppm (-$SCH_2\underline{CH_2}$ $(CH_2)_3$ CH_3), 31.91 ppm (-SCH_2 $(CH_2)_4$ CH_3), 107.90-159.12 ppm (Ar-C), 161.56 ppm (CH=N),164.85 ppm (C=O ester), 171.23 ppm (C=N thiazole); IR (cm^{-1}): 3057 (C-H aromatic), 2858-2953 (C-H aliphatic), 1732 (C=O ester), 1598 (CH=N),1573 (C=N thiazole); MS (ESI *m/z*) 493 [M^+].

(E)-4-(((6-fluorobenzo[d]thiazol-2-yl)imino) methyl)phenyl 4-(heptylthio)benzoate (F-SR7):

Chemical Formula: $C_{28}H_{27}FN_2O_2S_2$, yellow solid, yield:77.8 %; ^{1}H-NMR (400 MHz, $CDCl_3$) δ ppm: 0.87-0.91 (t,3H, $\underline{CH_3}$) ppm, 1.30-1.35 (m,6H, -$S(CH_2)_3\underline{(CH_2)_3}CH_3$) ppm,1.43-1.48 (P,2H,-$S(CH_2)_2$ $\underline{CH_2}$ $(CH_2)_3CH_3$) ppm, 1.69-1.74 (p,2H, -SCH_2 $\underline{CH_2}$ $(CH_2)_4CH_3$) ppm, 3.00-3.03 (t,2H, -$SCH_2(CH_2)_5CH_3$) ppm, 7.19-8.11 (m,11H,Ar-H) ppm, 9.05 (S,1H, CH=N, a) ppm; ^{13}C-NMR (400 MHz, $CDCl_3$) δ ppm: 14.11 ppm ($\underline{CH_3}$),22. 61 ppm (-$S(CH_2)_5\underline{CH_2}$ CH_3), 28.68 ppm (-$S(CH_2)_4\underline{CH_2}$ CH_2CH_3), 28.85 ppm (-$S(CH_2)_3\underline{CH_2}$ $(CH_2)_2CH_3$), 28.90 ppm (-$S(CH_2)_2\underline{CH_2}$ $(CH_2)_3CH_3$), 31.70 ppm (-$SCH_2\underline{CH_2}$ $(CH_2)_4CH_3$), 31.87 ppm (-SCH_2 $(CH_2)_5CH_3$), 107.92-159.11 ppm (Ar-C), 161.56 ppm (CH=N),164.88 ppm (C=O ester), 171.23 ppm (C=N thiazole); IR (cm^{-1}): 3057 (C-H

aromatic), 2856-2954 (C-H aliphatic), 1732 (C=O ester), 1598 (CH=N),1575 (C=N thiazole); MS (ESI *m/z*) 507 [M^+].

(E)-4-(((6- fluorobenzo[d]thiazol-2-yl)imino) methyl)phenyl 4-(octylthio)benzoate (F-SR8):

Chemical Formula: $C_{29}H_{29}FN_2O_2S_2$, yellow solid , yield:78 %; ^{1}H-NMR (400 MHz, $CDCl_3$) δ ppm: 0.87-0.88 (t,3H, $\underline{CH_3}$) ppm, 1.28 (m,8H,-$S(CH_2)_3\underline{(CH_2)_4}CH_3$) ppm, 1.45-1.47 (P,2H ,-$S(CH_2)_2$ $\underline{CH_2}$ $(CH_2)_4CH_3$) ppm, 1.65-1.72 (p,2H, -SCH_2 $\underline{CH_2}$ $(CH_2)_5CH_3$) ppm, 3.00-3.03 (t,2H, -SCH_2 $(CH_2)_6CH_3$) ppm, 7.19-8.11 (m,11H,Ar-H) ppm, 9.06 (S,1H, CH=N, a) ppm; ^{13}C- NMR (400 MHz, $CDCl_3$) δ ppm: 13.98 ppm ($\underline{CH_3}$),22.58 ppm (-$S(CH_2)_6\underline{CH_2}$ CH_3),28. 74 ppm (-$S(CH_2)_5\underline{CH_2}$ CH_2 CH_3),28.88 ppm (-$S(CH_2)_4\underline{CH_2}$ $(CH_2)_2CH_3$), 29.08 ppm (-$S(CH_2)_2$ $\underline{(CH_2)_2}$ $(CH_2)_3CH_3$), 31.74 ppm (-SCH_2 $\underline{CH_2}$ $(CH_2)_5CH_3$), 32.07 ppm (-SCH_2 $(CH_2)_6CH_3$), 107.82-159.31 ppm (Ar-C), 161.56 ppm (CH=N),164.74 ppm (C=O ester), 171.23 ppm (C=N thiazole); IR (cm^{-1}): 3057 (C-H aromatic), 2854-2953 (C-H aliphatic), 1734 (C=O ester), 1595 (CH=N),1575 (C=N thiazole); MS (ESI *m/z*) 521 [M^+].

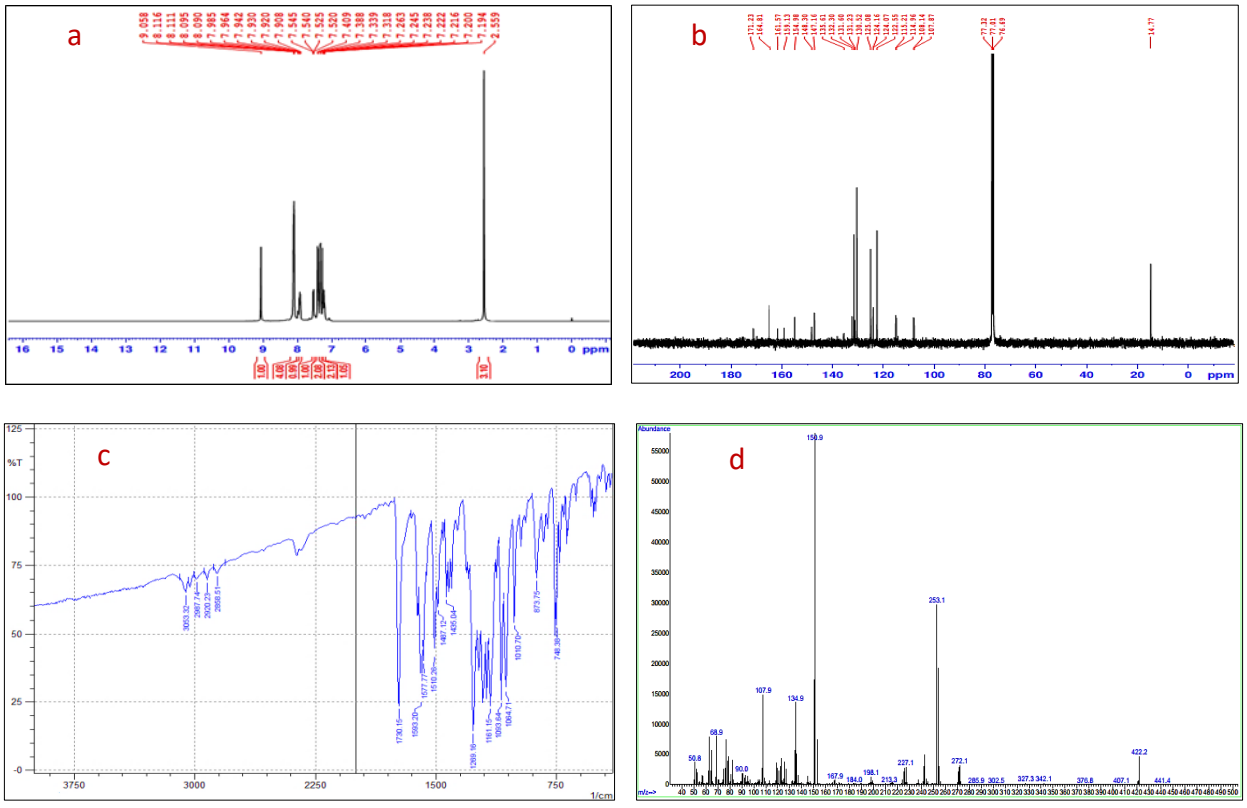

Figure 2. Represented the spectral methods represented with ^{1}H- NMR (a) ,^{13}C- NMR (b) , FT- IR (c), and Mass spectrum (d) of the compound (F-SR1).

RESULTS AND DISCUSSION

Chemistry

The compounds under study have a similar molecular structure except for a regular increase in the number of methylene groups in the thioalkyl series at one end of the molecules. The recently investigated compounds were manufactured by a three-step method. First, involved synthesizing thioalkyl benzoic acid from the reaction of 4-mercapto benzoic acid with alkylbromide [46]. Second, it entailed reacting 4-hydroxybenzaldehyde with 6-fluorobenzo[d]thiazol-2-amine zole to create benzo-thiazole imine bases. [48]. Third, it involved synthesizing the imine-ester of benzothiazole utilizing azomethene bases derived from the preceding step and thioalkyl benzoic acid (Scheme 1) [52]. The structures of the produced materials were verified using mass spectrometry, FT- IR, ^{1}H-NMR, and ^{13}C-NMR **(Supplementary materials S8-S35)**. POM and DSC were also used to investigate the liquid crystal materials' thermal mesomorphic characteristics.

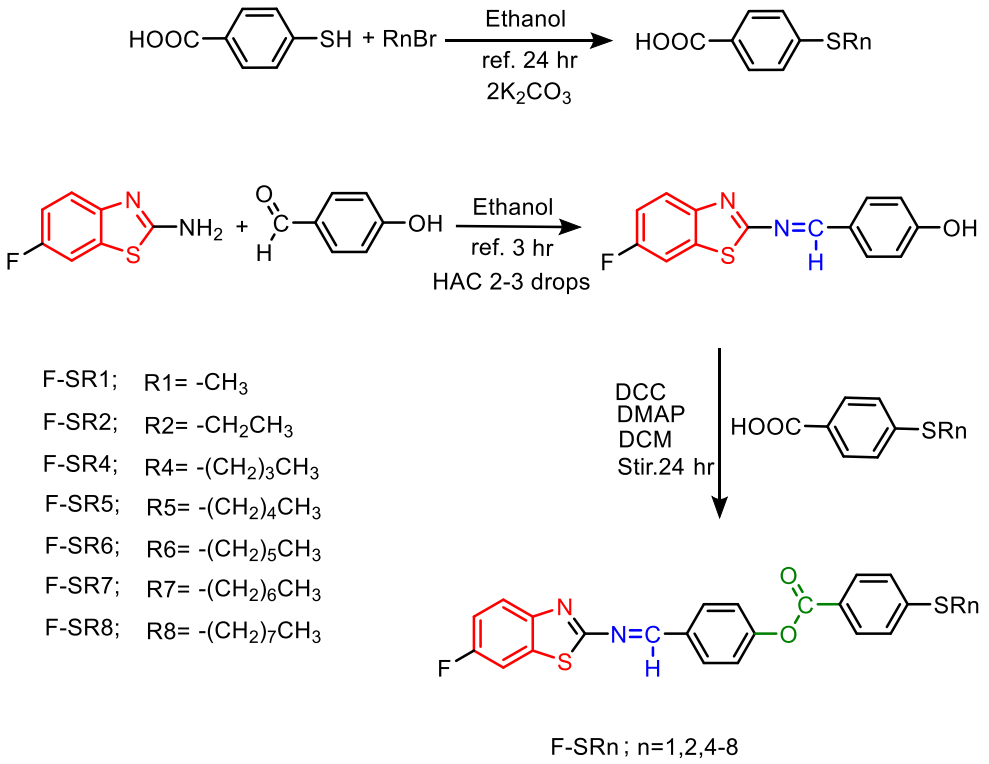

Scheme 1. General Scheme of the prepared compounds (F-SRn where n= 1,2,4-8)

Liquid Crystalline Investigations

The thermodynamic characteristics, textures, and examine the phase transitions of all prepared derivatives were specified by DSC **(supplementary materials S1-S7)** and POM. As shown in Table 1, the DSC heating data of the produced derivatives made it easier to determine the compounds' transition temperatures, corresponding enthalpy values (ΔH kJ/mol), and entropy changes (ΔS J/mol.K). The POM analysis provided images that validated the presence of smectic and nematic mesophases, contingent upon n, Figure 5.

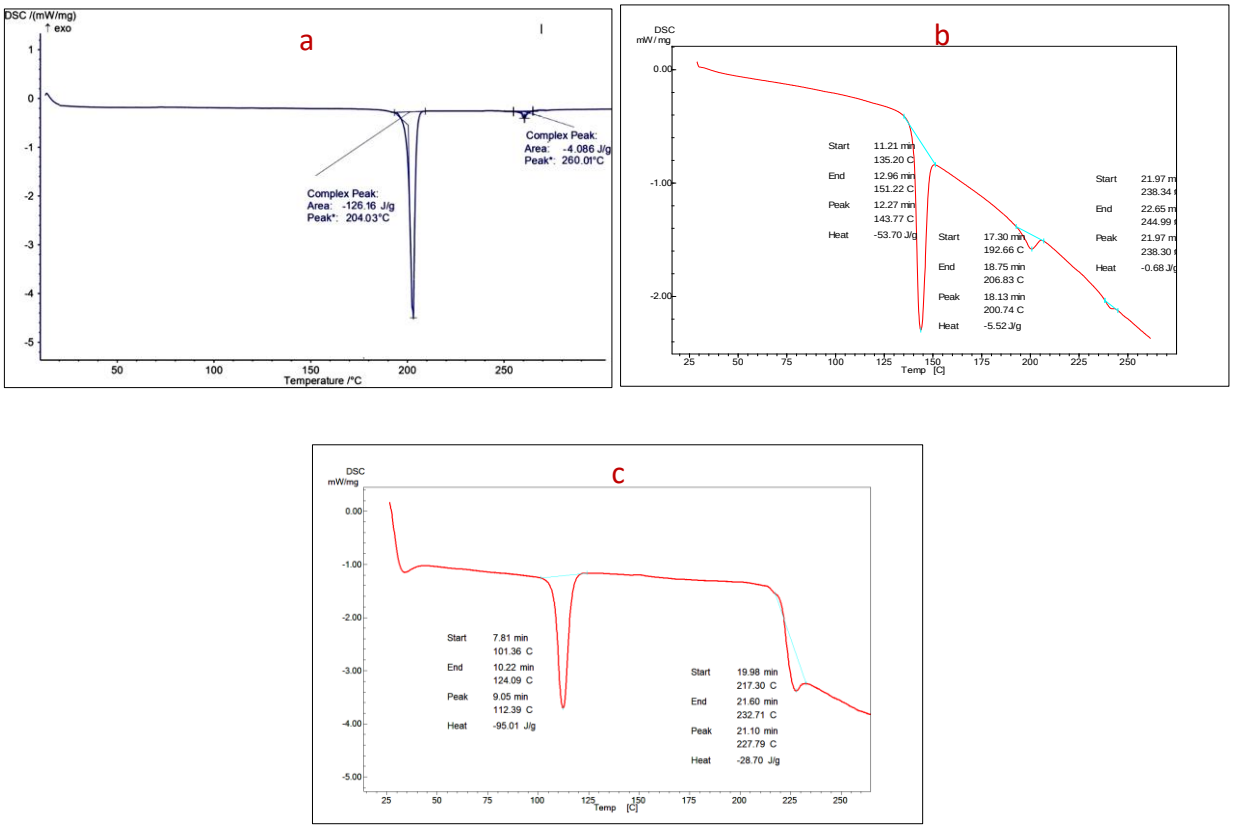

Figure 3. DSC thermograms of (a) F-SR1; (b) F-SR4; and (c) F-SR8 compounds.

Table 1. Transition temperatures (°C), (ΔH KJ/mol), (ΔS J/mol.K) and (ΔT_N , ΔT_{SmA}) of F-SRn.

Symbol	Transition Temp. (°C)	ΔH	ΔS	ΔT_{SmA} (°C)	ΔT_N (°C)
F-SR1	C→N 204.03 N→I 260.01	53.23 1.72	111.60 3.23	—	55.98
F-SR2	C→N 135.22 N→I 180.90	19.51 0.35	47.80 0.78	—	45.68
F-SR4	C→Sm 143.77 Sm→N 200.74 N→I 238.30	24.94 2.56 0.31	59.85 5.41 0.61	56.97	37.56
F-SR5	C→Sm 120.65 Sm→N 218.47 N→I 240.06	18.15 3.61 0.38	46.11 7.36 0.74	97.82	21.50

Symbol	Transition Temp. (°C)	ΔH	ΔS	ΔT_{SmA} (°C)	ΔT_N (°C)
F-SR6	C→Sm 123.20 Sm→N 223.22 N→I 235.02	34.18 3.87 0.74	86.29 7.81 1.47	100.02	11.80
F-SR7	C→Sm 116.49 Sm→I 225.50	13.37 6.25	34.34 12.55	109.01	—
F-SR8	C→Sm 112.39 Sm→I 227.79	49.46 14.94	128.36 29.83	115.40	—

C: Crystal , Sm, Smectic, N: Nematic , I: Isotropic , ΔT_N : Thermal range of the nematic phase, ΔT_{SmA} : Thermal range of the Smectic phase

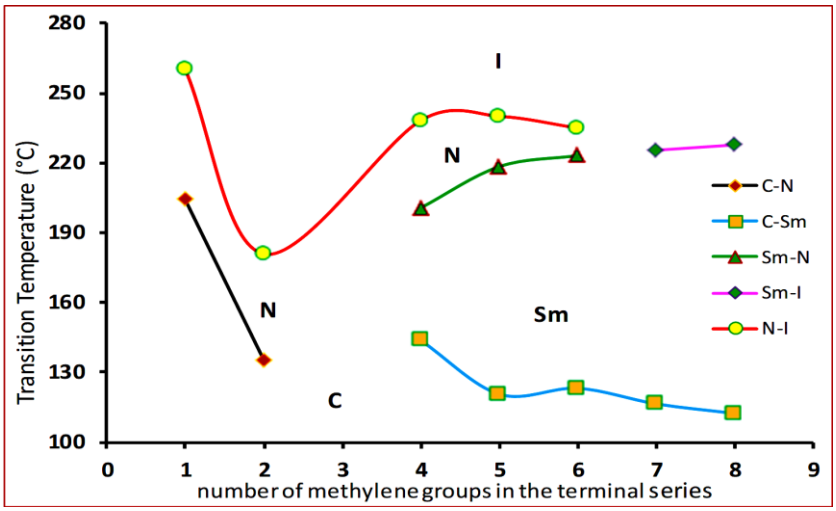

Figure 4. The relationship among transition temperatures and the number of methylene groups in the terminal series (F-SRn).

The findings displayed in Table 1 and (Figure 4) indicate that the fusion transitions exhibit an uneven pattern as the number of methylene groups in the terminal series increases (n = 1, 2, 4-8). The melting temperatures correlate with the polarizability and molecular configuration of the synthesized compounds [53,54]. The two compounds F-SR1 (Figure 3a), F-SR2 showed only the nematic phase (short thioalkyle chain). The temperature range in compound F-SR1 (55.98°C) was wider than that in compound F-SR2 (45.68°C). While compounds with medium-length terminal chains F-SR4 (Figure 3b), F-SR5, F-SR6 exhibited both smectic and nematic phases with different thermal ranges [55]. As for Compounds with long terminal chain F-SR7, F-SR8 (Figure 3c) exhibited only the smectic phase, with a higher temperature range than in compounds (F-SR4, F-SR5, F-SR6) [56]. The variation in the behavior of compounds within the series (F-SRn where

n=1,2,4-8) is explained by the fact that in liquid crystals systems there is a equilibrium among the intermolecular interactions at the sides of the molecules (lateral attractive forces) and the interactions at the ends of the molecules (terminal attractive forces). But this balance is disrupted when there is a change in the length or width of the molecule, and as affect the thermal range of the nematic or smectic phase is affected [57,58]. The compounds prepared in this series have a constant molecular structure except for a regular rise in the number of methylene groups in the thioalkyl chain at one end of the molecules. This means the change occurs in the length of the molecule while the width remains constant. Growing the length of the terminal chain leads to two opposing belongings: First, an increase in lateral attractive forces, and the second is a decrease in terminal attractive forces because of augmented parting between the ends of the particles containing polar groups, in addition to increased flexibility [6]. The type of mesophase that appears in liquid crystal composites be contingent on the relation of terminal to lateral attractive militaries. This ratio is high in short thioalkyl chains, enhancing the arrival of the nematic stage [59]. This is what was identified in compounds (F-SR1, F-SR2). However, with an increase in chain length, this ratio decreases, which gives the possibility of the molecules taking a layered arrangement, which enhances the appearance of the smectic stage in adding to the nematic phase, as in compounds (F-SR4, F-SR5, F-SR6). As chain length increases, this ratio decreases further. Consequently, the nematic stage disappears, and just the smectic phase appears, as in compounds (F-SR7, F-SR8), with a reduction in the temperature range of the nematic phase and an increase in the thermal range of the smectic phase [6,28].

Generally, the molecular shape, aspect-ratio, molecular rigidity ,energy gap, dipole moment, and polarizability of the examined system are significantly influenced by the electronic characteristics of the connected terminal collections. Furthermore, the characteristics of the liquid crystals are affected by an increasing in the polarity and/or polarization state of the mesogenic segments [58,60,61].

In the current work, compounds F-SR1, F-SR2, F- SR4, F- SR5, and F- SR6 are sequenced based on the $\langle \Delta T_N \rangle$ values of their nematic phase:

F-SR1 > F-SR2 > F-SR4 > F-SR5 > F-SR6

ΔT_N (°C): 55.98 45.68 37.56 21.50 11.80

While compounds F-SR4, F-SR5, F-SR6, F-SR7, and F-SR8 are sequenced based on the $\langle \Delta T_{SmA} \rangle$ values of their smectic phase:

F-SR4 < F-SR5 < F-SR6 < F-SR7 < F-SR8

ΔT_{SmA} (°C) : 56.97 97.82 100.02 109.01 115.40

The POM analysis provided images that validated the presence of smectic and nematic mesophases (Figure 5) contingent upon n [58].

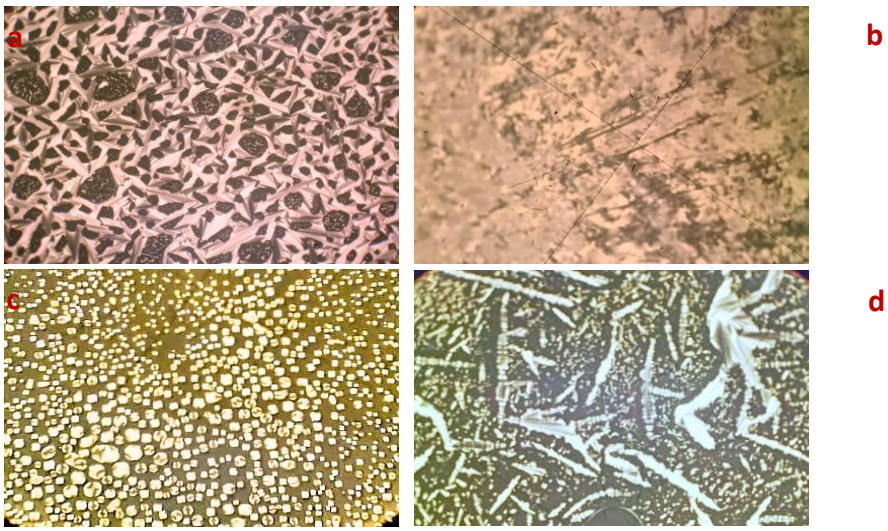

Figure 5. POM textures (a) SmA phase in heating; (b) N phase in heating; (c) SmA phase in cooling and (d) N phase in cooling.

Analysis benzothiazole derivatives theoretically

Molecule orbital characteristics, dipole moments, thermodynamic parameters, and molecule electrostatic characteristics are highlighted by computer-aided quantum mechanical techniques. The composites' different characteristics were predicted and their structure in the gas phase was optimized using the DFT approach. The CAM-B3LYP functional was applied using the Gaussian 09 suite with a 6–311G (2d,p) basis set [62]. This theoretical framework, which is widely used in computer analyses, produces exact geometric configurations and the frequencies of normal modes. The dipole moment, the energy of the highest occupied molecular orbital (E_{HOMO}), the energy of the lowest unoccupied molecular orbital (E_{LUMO}), chemical hardness ⟨η⟩, and chemical softness ⟨S⟩ were all calculated using formulas [52,63,64]. Optical softness ⟨So⟩, Thus, electron affinity ⟨EA⟩ and ionization potential ⟨I.P.⟩ for the for the examined substances. (Figure 6) illustrates the geometric optimizations along with the dimensions of the analyzed.

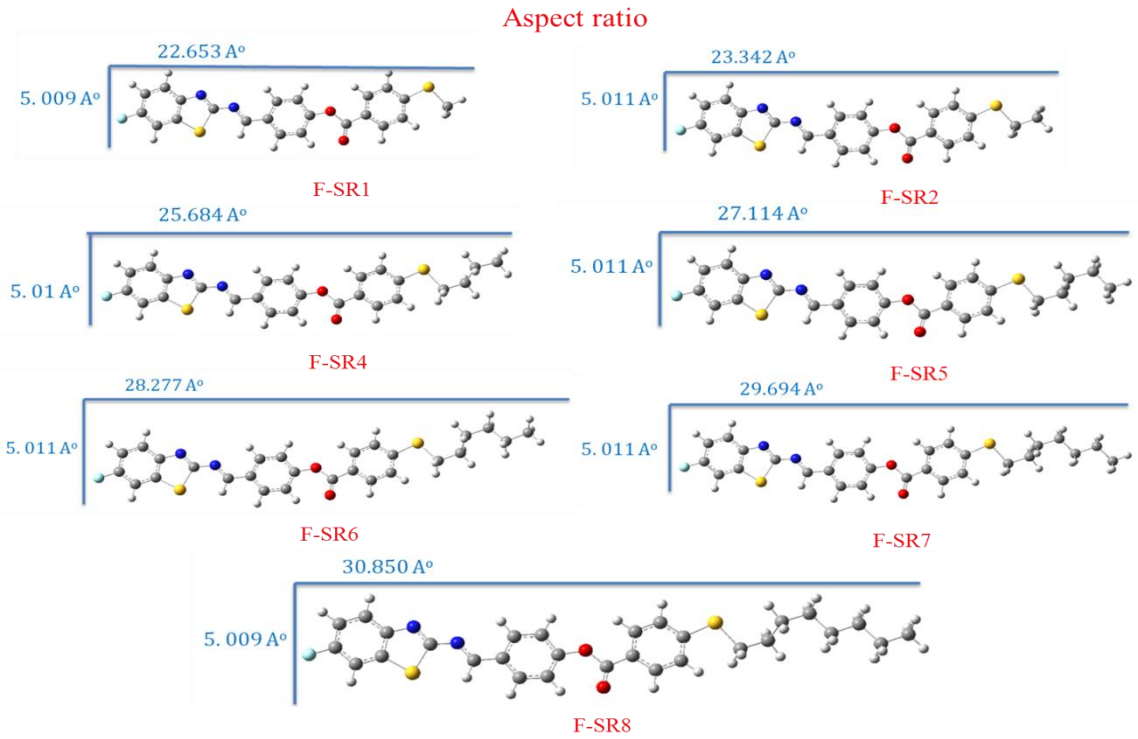

Figure 6. The dimensions and optimized molecular geometries of the investigated F-SRn members.

The calculated dipole moment (**μ**) and aspect ratio values from this theoretical investigation elucidate the spotted variances in the temperature characteristics of the members, as presented in Table 2. The dipole moment (**μ**) values presented in (Figure 7) ordered these members in the subsequent order:

F- SR1 < F- SR2 < F- SR4 < F- SR5 < F- SR6 < F- SR7 < F- SR8

(**μ**) : 6.01 6.76 6.87 6.98 7.06 7.11 7.19

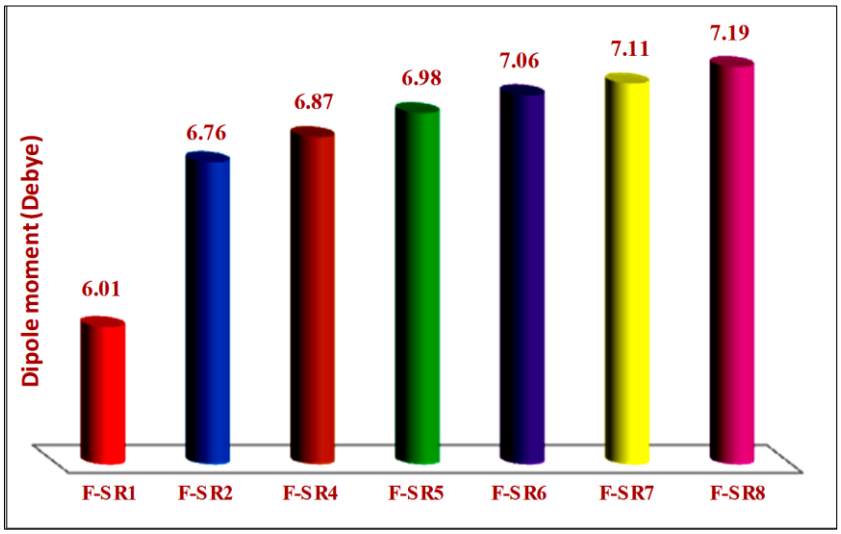

Figure 7. The theoretically computed total dipole moment values for the examined substances

The relationship between the calculated aspect ratio and the (ΔT) values of the studied compounds is illustrated (Figures 8 and 9). The compounds were organized in the subsequent sequence based on the increase in their aspect ratio, as shown in Table 2:

F-SR1 < F-SR2 < F-SR4 < SR5 < F-SR6 < F-SR7 < F-SR8

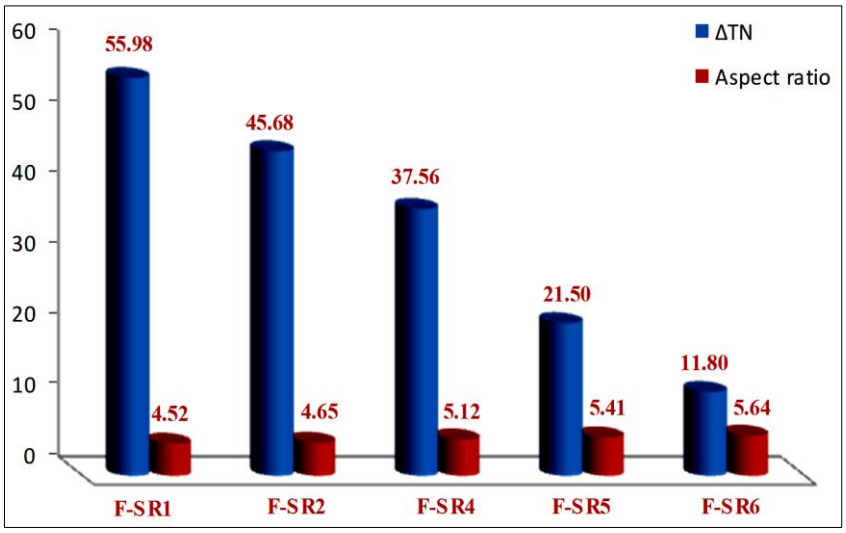

Figure 8. The theoretical relationship between the thermal range (ΔT_N) of the examined compounds F-SR1,F-SR2,F-SR4,F-SR5, and F-SR6 and their aspect ratio was assessed.

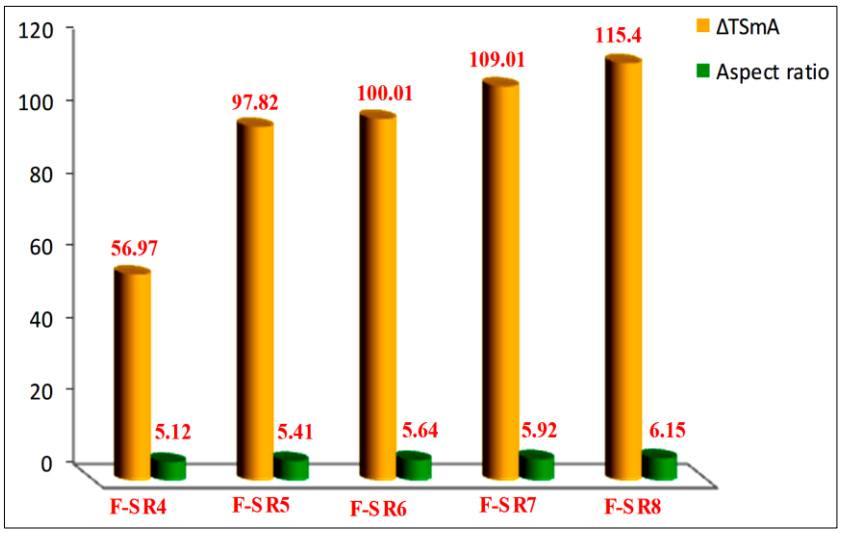

Figure 9. The theoretical relationship between the thermal range (ΔT_{SmA}) of the examined compounds F-SR4, F-SR5, F-SR6, F-SR7, and F-SR8 and their aspect ratio was conducted.

Table 2. Etot, dipole Moment (Debye) , and aspect ratio of the substances under study.

Parameter	F-SR1	F-SR2	F-SR4	F-SR5	F-SR6	F-SR7	F-SR8
Etot	-2003.174093	-2042.479568	-2121.087047	-2160.389756	-2199.693778	-2238.997929	-2278.301998
Dipole moment (D)	6.0190	6.764	6.877	6.985	7.066	7.118	7.193
Aspect ratio	4.5224	4.6581	5.1265	5.4108	5.6429	5.9257	6.1589

Frontier Molecular Orbitals (FMOs)

The HOMO and LUMO are indicated by frontier molecular orbitals (FMOs). The HOMO serves as a donor of electrons. By taking in electrons, the LUMO performs the role of an electron acceptor. They could demonstrate a rational qualitative forecast of electron conveyance capability through the excitement of electrons from the HOMO to the LUMO [65]. (Figure 10) shows the projected ground state density surface plots for the FMOs of the present groups F-SRn. Table 3 compiles the FMO energy gap results. Where, the electron densities of the places that donate to the creation of the HOMOs and the LUMOs are localized on each of the imine linkage and the thiazol ring. Furthermore, the length of the thioalkyl chain (n) has a slight effect on the energy gap of frontier molecular orbitals. According to a publication [66], the conjugation inside the mesogenic cores and the expanded terminal chain significantly reduce the FMO energy gap. Moreover, the chemical reactivity of molecules is determined by the energy gap (ΔE) between the HOMO and LUMO states [67]. A lower number suggests that the chemical is more reactive. According to (Table 3) predicted energy gap, the F-SR8 molecule is more reactive than the others. Since the energy gap is directly proportional to hardness and inversely correlated with softness, it is softer and less hard than others. Molecular interactions, which essentially depend on the molecular geometry of the produced compounds, the polarizability of the terminals and substituents, and the stereoelectronic characteristics of the entire molecule, are influenced by the mesomorphic behavior of rod-like mesogens.

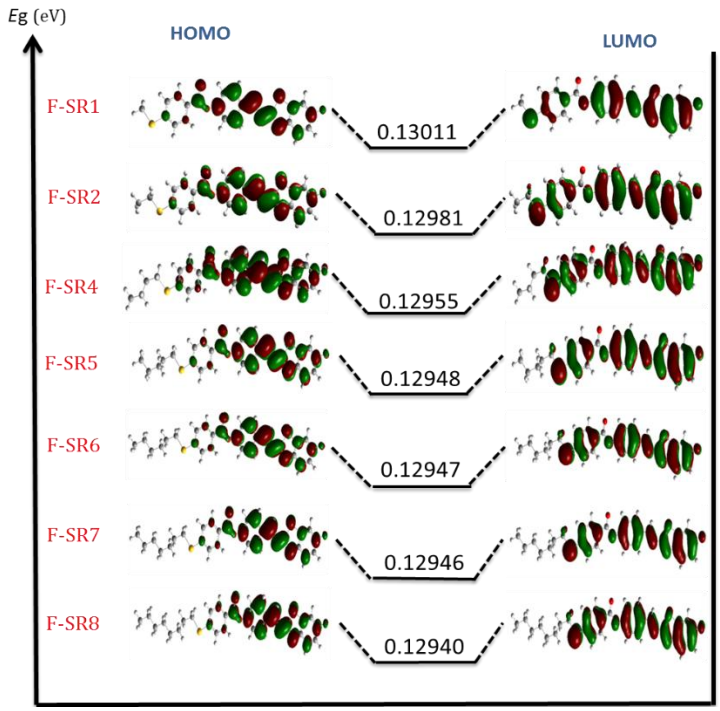

Figure 10. HOMO, LUMO, and *E*g in electron volts for the examined compounds.

Table 3. The HOMO, LUMO, and several CQDs of the investigated compounds.

Compound	E_{HOMO} (eV)	E_{LUMO} (eV)	E_{gap} (eV)	IE = - E_{HOMO}	EA= - E_{LUMO}	η=IE-EA/2	S = 1/η	So = S/2
F-SR1	-0.22645	-0.09634	0.13011	0.22645	0.09634	0.065055	15.3716086	7.685804319
F-SR2	-0.22567	-0.09586	0.12981	0.22567	0.09586	0.064905	15.4071335	7.703566751
F-SR4	-0.22524	-0.09569	0.12955	0.22524	0.09569	0.064775	15.4380548	7.719027403
F-SR5	-0.22507	-0.09559	0.12948	0.22507	0.09559	0.06474	15.446401	7.723200494
F-SR6	-0.22505	-0.09558	0.12947	0.22505	0.09558	0.064735	15.447594	7.723797019
F-SR7	-0.22506	-0.09560	0.12946	0.22506	0.09560	0.064730	15.4487873	7.724393635
F-SR8	-0.22500	-0.09560	0.12940	0.22500	0.09560	0.064700	15.4559505	7.727975270

$S(eV^{-1})$ = Softness, So (eV^{-1}) = Optical softness, (IE) (eV) = Ionization potential, (EA) (eV)= Electron affinity, η (eV) = Hardness

Analysing the electrostatic surface potential (ESP)

Mesomeric arrangements, which are often altered by intermolecular interactions, have an impact on the molecular conformation of the synthesized LC members. The electron density delivery at atomic locations of LC compounds influences their electronic construction, polarizability, dipole moment, and other various [68]. Molecular electrostatic potential (MEP) is a excellent method for predicting the inter- or intra-molecular between the prepared molecules. MEP is a metric that illustrates how the electron density is distributed inside the molecule framework. Using the CAM- B3LYP /6-311G (2d,p) methodology in accordance with MEP, the charge distribution map for the members under examined (F-SRn) was computationally projected, Figure 11.

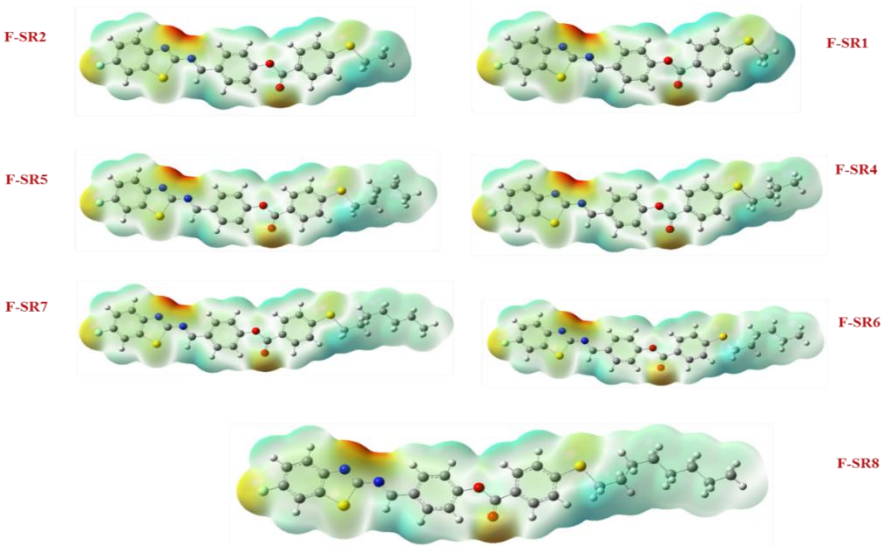

Figure 11. The members under examination's electrostatic surface potential (ESP).

The MEP studies indicate elevated electrostatic potential yet diminished electron density for the terminal polar thioalkyl groups of all synthesized components (F-SRn); this is illustrated by the blue cloud. Conversely, the red patches, indicative of top electron density, are anticipated to be concentrated on the mesogenic cores, namely at the oxygen atoms of the ester linkage, the sulfur atom of the thioalkyl chains, the nitrogen atoms of

each Schiff base linkage, and the thiazol ring. Furthermore, the terminal F atom exhibited negligible negatively charged locations, depicted as yellow areas.

CONCLUSION

Fundamental Finding : The mesophase begins to develop in the lowest member (F-SR1), characterized by the broadest nematic stage width, suggesting that the existing structure possesses an effective mesogenic core for mesophase production. In short thioalkyl chains, the nematic phase appears, and this phase was identified in compounds F-SR1 and F-SR2. However, with increasing chain length, both the smectic and nematic phases appear, as in compounds F-SR4, F-SR5, and F-SR6. With further increases in chain length, only the smectic phase appears, as in compounds F-SR7 and F-SR8. The experimental results are consistent with the theoretical findings for these compounds. **Implication :** These consequences profoundly influence our coming trajectory by utilizing the existing core system for the expansion of novel liquid crystal molecules. DFT simulations showed that changes in the terminal thioalkyl enhanced the thermodynamic energy as well as the geometrical parameters and mesomorphic phase stability. **Limitation :** Availability of data and material: The datasets used and analyzed during the current study are available from the corresponding author on reasonable request. **Future Research :** This work details the Preparation process and liquid crystal characteristics of homologous series of (F-SRn, where n=1,2,4-8).

REFERENCES

[1] D.-K. Yang and S.-T. Wu, Fundamentals of Liquid Crystal Devices. Hoboken, NJ, USA: John Wiley & Sons, 2014.

[2] I. Dierking and S. Al-Zangana, "Lyotropic liquid crystal phases from anisotropic nanomaterials," Nanomaterials, vol. 7, no. 10, p. 305, 2017, doi: 10.3390/nano7100305.

[3] N. S. Al-Kadhi et al., "Novel imidazole liquid crystals: Experimental and computational approaches," Molecules, vol. 27, no. 14, p. 4607, 2022, doi: 10.3390/molecules27144607.

[4] F. S. Alamro et al., "Physical and thermal characterizations of newly synthesized liquid crystals based on benzotrifluoride moiety," Materials, vol. 16, no. 12, p. 4304, 2023, doi: 10.3390/ma16124304.

[5] D. Demus et al., Handbook of Liquid Crystals. Weinheim, Germany: VCH-Wiley, 1998.

[6] G. W. Gray, Molecular Structure and the Properties of Liquid Crystals. London, UK: Academic Press, 1962.

[7] B. T. Thaker et al., "Synthesis and mesomorphic investigations of liquid crystalline compounds having a benzothiazole ring," Mol. Cryst. Liq. Cryst., vol. 575, no. 1, pp. 64–76, 2013, doi: 10.1080/15421406.2013.766947.

[8] J. F. Johnson and R. S. Porter, Liquid Crystals and Ordered Fluids. New York, NY, USA: Plenum Press, 1970.

[9] G. Smith, Advances in Liquid Crystals. New York, NY, USA: Academic Press, 1975.

[10] P. G. de Gennes, The Physics of Liquid Crystals. Oxford, UK: Clarendon Press, 1975.

[11] G. W. Gray, Thermotropic Liquid Crystals. New York, NY, USA: Wiley, 1987.

[12] S. Chandrasekhar, Liquid Crystals. Cambridge, UK: Cambridge Univ. Press, 1977.

[13] P. Rene, A. S. Jorg, and T. Carsten, "Synthesis and thermotropic liquid crystalline properties…," J. Mater. Chem., vol. 8, pp. 2611–2626, 1998, doi: 10.1039/A803043J.
[14] T. H., M. T., K. I., K. K., A. M., and Y. F., "Solid-phase synthesis of liquid crystalline isoxazole library," Tetrahedron Lett., vol. 45, pp. 2277–2279, 2004, doi: 10.1016/j.tetlet.2004.01.116.
[15] S. T. Ha et al., "Mesogenic Schiff base esters," Int. J. Phys. Sci., vol. 5, pp. 564–575, 2010.
[16] S. T. Ha, G. Y. Yeap, and P. L. Boey, "Synthesis and smectogenic properties…," Int. J. Phys. Sci., vol. 5, pp. 182–191, 2010.
[17] C. Y. Chang et al., "Synthesis of laterally substituted α-methylstilbene-tolane liquid crystals," Liq. Cryst., vol. 35, pp. 1–9, 2008.
[18] U. J. Al-Hamdani, "Mesomorphic properties of an homologous series," Int. J. Mol. Sci., vol. 12, no. 5, pp. 3182–3190, 2011, doi: 10.3390/ijms12053182.
[19] G. Fornasieri, F. Guittard, and S. Géribaldi, "Influence of the structure," Liq. Cryst., vol. 30, no. 2, pp. 251–257, 2003.
[20] U. J. Al-Hamdani et al., "Synthesis, mesomorphic properties," Liq. Cryst., vol. 48, no. 15, pp. 2164–2177, 2021.
[21] A. S. Matharu and D. Chambers-Asman, "Structure-property investigation," Liq. Cryst., vol. 34, pp. 1317–1336, 2007.
[22] H. Gallardo et al., "Synthesis, characterization and mesomorphic properties," Liq. Cryst., vol. 28, pp. 1343–1352, 2001.
[23] A. Seed, "Synthesis of self-organizing mesogenic materials," Chem. Soc. Rev., vol. 36, pp. 2046–2069, 2007.
[24] L. L. Lai et al., "Synthesis and characterization," Mol. Cryst. Liq. Cryst., vol. 287, pp. 177–181, 1996.
[25] W. Weisswange, Ph.D. dissertation, Univ. Halle, Germany, 1925.

[26] U. J. Al-Hamdani et al., "Chloro-benzothiazole Schiff base ester liquid crystals," Liq. Cryst., vol. 49, no. 13, pp. 1866–1877, 2022.
[27] B. T. Thaker et al., "Mesomorphic studies of novel azomesogens," Liq. Cryst., vol. 40, no. 2, pp. 237–248, 2013.
[28] K.-L. Foo et al., "Mesomorphic behaviors," Phase Transitions, vol. 92, no. 1, pp. 87–99, 2019.
[29] D. Demus et al., "Phase structures of calamitic liquid crystals," in Handbook of Liquid Crystals, vol. 2A, Wiley-VCH, 1998, pp. 3–23.
[30] R. J. Bushby and O. R. Lozman, "Discotic liquid crystals 25 years on," Curr. Opin. Colloid Interface Sci., vol. 7, pp. 343–354, 2002.
[31] L. R. Savagian et al., "Balancing charge storage and mobility," Adv. Mater., vol. 30, no. 50, 2018.
[32] A. F. Paterson et al., "Recent progress in high-mobility organic transistors," Adv. Mater., vol. 30, no. 36, 2018.
[33] J. Chin and H. J. Kim, "Near-infrared fluorescent probes," Coord. Chem. Rev., vol. 354, pp. 169–181, 2018.
[34] G. G. Dias et al., "Quinone-based fluorophores," Chem. Soc. Rev., vol. 47, no. 1, pp. 12–27, 2018.
[35] J.-M. Lehn, "Toward self-organization and complex matter," Science, vol. 295, no. 5564, pp. 2400–2403, 2002.
[36] V. V. Titov and A. I. Pavlyuchenko, "Thermotropic liquid crystals in the heterocyclic series," Chem. Heterocycl. Compd., vol. 16, no. 1, pp. 1–13, 1980.

[37] A. A. Zaki, H. A. Ahmed, and M. Hagar, "Impact of fluorine orientation," Mater. Chem. Phys., vol. 216, pp. 316–324, 2018.
[38] M. Lehmann et al., "High charge-carrier mobility," Chem. Eur. J., vol. 11, no. 11, pp. 3349–3362, 2005.
[39] M. Takase et al., "Annularly fused hexapyrrolohexaazacoronenes," Angew. Chem. Int. Ed., vol. 46, no. 29, pp. 5524–5527, 2007.
[40] H. A. Ahmed, M. Hagar, and O. A. Alhaddad, "Experimental and theoretical approaches," Liq. Cryst., vol. 46, no. 9, pp. 1440–1451, 2019.
[41] H. A. Ahmed et al., "Wide nematic phases induced by hydrogen-bonding," Liq. Cryst., vol. 46, no. 4, pp. 550–559, 2019.
[42] H. A. Ahmed, M. Hagar, and A. Aljuhani, "Mesophase behavior of new linear supramolecular complexes," RSC Adv., vol. 8, pp. 34937–34946, 2018.
[43] H. A. Ahmed et al., "Phase behavior and DFT calculations," Crystals, vol. 9, no. 3, p. 133, 2019.
[44] E. Cruickshank et al., "Helical phases assembled from achiral molecules," J. Mol. Liq., vol. 346, p. 118180, 2022.
[45] U. J. Al-Hamdani et al., "Effects of terminal substituents," Liq. Cryst., vol. 49, no. 14, pp. 1998–2007, 2022.
[46] U. J. Al-Hamdani, "Mesomorphic properties of an homologous series of thioalkyl-terminated azomesogens," Int. J. Mol. Sci., vol. 12, pp. 451–460, 2011.
[47] S. Nada et al., "Three rings Schiff base ester liquid crystals: experimental and computational approaches," Molecules, vol. 27, no. 7, p. 2304, 2022.
[48] O. A. Alhaddad et al., "Mesophase behavior of four ring ester/azomethine/ester liquid crystals," Liq. Cryst., vol. 49, no. 10, pp. 1395–1402, 2022.
[49] U. J. Al-Hamdani et al., "Thermal nonlinearity and all-optical switching of synthesized Azo-Cl compound," Opt. Mater., vol. 139, p. 113824, 2023.
[50] U. J. Al-Hamdani et al., "Synthesis and investigation of nonlinear optical properties of Azo-SR8 compound," Opt. Mater., vol. 143, p. 114293, 2023.
[51] A. A. Fahmi et al., "Steric effect of di-lateral methyl substituent," Liq. Cryst., vol. 49, no. 11, pp. 1511–1523, 2022.
[52] U. J. Al-Hamdani et al., "Synthesis of Azo-BE: nonlinear optical properties studies," Opt. Quantum Electron., vol. 56, no. 7, p. 1276, 2024.
[53] M. Karthikeyan, R. C. Glen, and A. Bender, "General melting point prediction," J. Chem. Inf. Model., vol. 45, pp. 581–590, 2005.
[54] F. S. Alamro et al., "Synthesis, phase behavior and computational simulations," Molecules, vol. 26, no. 21, p. 6416, 2021.
[55] F. S. Alamro et al., "Physical and thermal characterizations," Materials, vol. 16, no. 12, p. 4304, 2023.
[56] N. A. S. Zulaziz, Z. Jamain, and M. Khairuddean, "Synthesis, characterization, and liquid crystalline behavior," Malays. J. Chem., vol. 26, pp. 572–582, 2024.
[57] M. J. Shirodkar et al., "Mesomorphic and DFT study of new difluoro substituted Schiff base liquid crystals," Sci. Rep., vol. 15, no. 1, p. 15540, 2025.
[58] V. Chemi, Texture of Liquid Crystals. Weinheim, Germany: Wiley, 1978.
[59] F. S. Alamro et al., "Experimental and theoretical investigations of three-ring ester/azomethine materials," Materials, vol. 15, no. 6, p. 2312, 2022.

[60] F. S. Alamro et al., "Induced nematic phase of new synthesized laterally fluorinated azo/ester derivatives," Molecules, vol. 26, no. 15, p. 4546, 2021.
[61] F. S. Alamro et al., "Mesophase behavior of molecules containing three benzene rings…," ACS Omega, vol. 9, no. 29, pp. 31601–31610, 2024.
[62] D. A. Paterson et al., "Understanding the twist-bend nematic phase," Soft Matter, vol. 12, pp. 6827–6840, 2016.
[63] D. D. Sarkar et al., "Cholesterol-based dimeric liquid crystals," Liq. Cryst., vol. 40, pp. 468–481, 2013.
[64] U. J. Al-Hamdani et al., "Optical nonlinear properties and all optical switching," J. Mol. Liq., vol. 361, p. 119676, 2022.
[65] M. E. Elshakre et al., "On the role of the electronic states of corrosion inhibitors," Corros. Sci., vol. 124, pp. 121–130, 2017.
[66] M. S. Khushaim et al., "Experimental and computational simulations of nematogenic liquid crystals," Liq. Cryst., 2021.
[67] S. A. Popoola, A. R. Almohammedi, and K. Haruna, "Spectroscopic and DFT evaluation," Chem. Pap., vol. 75, no. 6, pp. 2775–2789, 2021.
[68] M. A. El-Atawy et al., "New nitro-laterally substituted azomethine derivatives," Molecules, vol. 26, p. 1927, 2021.

***Nizar S. Nwyr (Corresponding Author)**
University of Basrah, Iraq
Email: nzarshatynwyr@gmail.com

Uhood J. Al-Hamdani
University of Basrah, Iraq

Tahseen A. Alsalim
University of Basrah, Iraq